

See discussions, stats, and author profiles for this publication at: <https://www.researchgate.net/publication/5926033>

# Reticular Synthesis of Microporous and Mesoporous 2D Covalent Organic Frameworks

ARTICLE *in* JOURNAL OF THE AMERICAN CHEMICAL SOCIETY · NOVEMBER 2007

Impact Factor: 12.11 · DOI: 10.1021/ja0751781 · Source: PubMed

---

CITATIONS

303

---

READS

59

5 AUTHORS, INCLUDING:



**Hani M El-Kaderi**

Virginia Commonwealth University

42 PUBLICATIONS 2,180 CITATIONS

SEE PROFILE



**Hiroyasu Furukawa**

University of California, Los Angeles

81 PUBLICATIONS 11,139 CITATIONS

SEE PROFILE

## Reticular Synthesis of Microporous and Mesoporous 2D Covalent Organic Frameworks

Adrien P. Côté,\* Hani M. El-Kaderi, Hiroyasu Furukawa, Joseph R. Hunt, and Omar M. Yaghi\*  
Center for Reticular Chemistry, Department of Chemistry and Biochemistry, University of California, Los Angeles,  
607 East Charles E. Young Drive, Los Angeles, California 90095

Received July 11, 2007; E-mail: apcote@chem.ucla.edu; yaghi@chem.ucla.edu

Reticular chemistry is concerned with linking molecular building blocks into predetermined periodic structures using strong bonds.<sup>1</sup> This chemistry has led to the design and synthesis of new porous materials for which the composition, structure, metrics, and functionality can be systematically varied.<sup>2,3</sup> The general nature of this approach is epitomized by the recent reports of covalent organic frameworks (COFs) in which the building blocks are linked by strong covalent bonds (C–C, C–O, B–O).<sup>4,5</sup> The successful crystallization of COFs indicates that it is possible to overcome the long standing “crystallization problem” for covalently linked solids. This is accomplished by striking a balance between the kinetic and thermodynamic factors that play in reversible covalent bond formation, a necessary criterion to crystallize extended structures. Here, we show the general utility and applicability of reticular chemistry to the systematic design of composition, structure, and porosity of three new layered COFs having pore sizes ranging 9–32 Å.

Co-condensation reactions between 2,3,6,7,10,11-hexahydroxytriphenylene (HHTP) and 1,3,5-benzenetriboronic acid (BTBA), 1,3,5-benzenetris(4-phenylboronic acid) (BTPA), and 4,4'-biphenyldiboronic acid (BPDA) produced COF-6, -8, and -10, respectively, with chemical formulas of  $C_8H_3BO_2$  (COF-6),  $C_{14}H_7BO_2$  (COF-8), and  $C_6H_3BO$  (COF-10). Upon condensation,  $C_2O_2B$  boronate esters were expected to form, thereby linking HHTP with BTBA (COF-6), BTPA (COF-8), and BPDA (COF-10) (Figure 1). Reactions were carried out in glass vials using 1:1 v/v solutions of mesitylene dioxane and heating at 85 °C for 48–120 h. Yields were 65–76% based on HHTP.<sup>6</sup> Spectroscopic analyses similar to that performed on the first COFs<sup>4,5</sup> (FT-IR, <sup>11</sup>B and <sup>13</sup>C MAS NMR) of the microcrystalline powders confirmed the formation of  $C_2O_2B$  rings and elemental microanalysis matched the expected COF compositions (see Supporting Information).

Linking trigonal-planar building blocks in the manner described above was expected to give planar hexagonal sheets, which upon crystallization can stack within two possibilities: graphite (**gra**,  $P6_3/mmc$ ) where layers are “slipped” or boron nitride (**bnn**,  $P6mm$ ) where layers are “eclipsed”.<sup>7</sup> Given these design parameters, we modeled the possible crystal structures that could form between HHTP and boronic acid building blocks (Figure 1).<sup>8</sup> Simulated powder X-ray (Cu K $\alpha$ ) diffraction patterns (PXRD) were calculated from the models and compared to those collected from reaction products (Figure 2). In all cases, COFs crystallized as eclipsed structures with hexagonally aligned 1D pores as identified by the near-perfect correspondence between peak positions and intensities between calculated and experimental PXRD patterns (Figure 2). Numerical fitting of PXRD patterns using the model-biased Le Bail method rigorously authenticated the unit cell parameters and atomic positions of models (Figure 2).<sup>9</sup> We note that our procedure of design and structural characterization can easily be applied to any material constructed from rigid molecular building blocks.

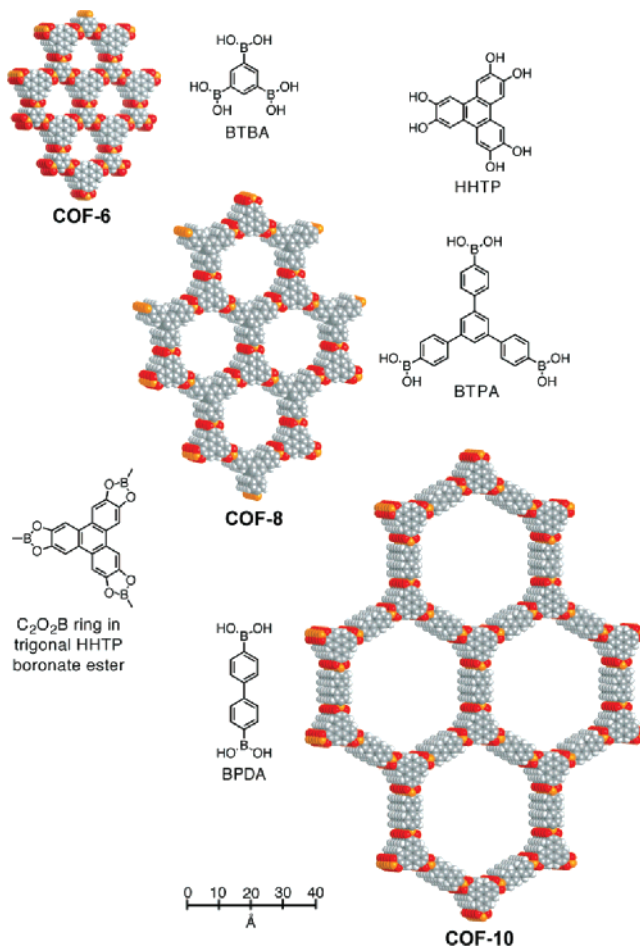


**Figure 1.** Co-condensation of boronic acid building blocks (BTBA, BTPA, BPDA) with HHTP to give 2D COFs (COF-6, -8, and -10) having systematically designed porous structures. COF illustrations are to scale. Coloring scheme: C, gray; H, white; B, orange; O, red.

COFs-6, -8, and -10 crystallize as 0.5–3.0  $\mu m$  hexagonal platelets (SEM), and small crystallites contribute significantly to the line broadening in PXRD patterns. The presence of (001) peaks indicates that 2D COFs are periodic in all three dimensions. The distance between layers directly relates to  $d_{001}$  and is consistently 3.4–3.6 Å, indicating close  $\pi$ – $\pi$  stacking between layers. This is likely assisted by distal dative interactions between boron and oxygen lone pairs of  $C_2O_2B$  groups on adjacent layers. The greater breadth of  $d_{001}$  peaks point to stacking faults between layers.<sup>10</sup>

Thermogravimetric analysis of COFs-6, -8, -10 shows that they are stable up to 450 °C. They are insoluble in common organic solvents such as alkanes, alcohols, acetone, and *N,N*-dimethylformamide. Crystalline COFs have a gray color arising from starting materials, including highly colored oxidized HHTP, that are included within the pores. Soaking crystals in acetone for 48–72

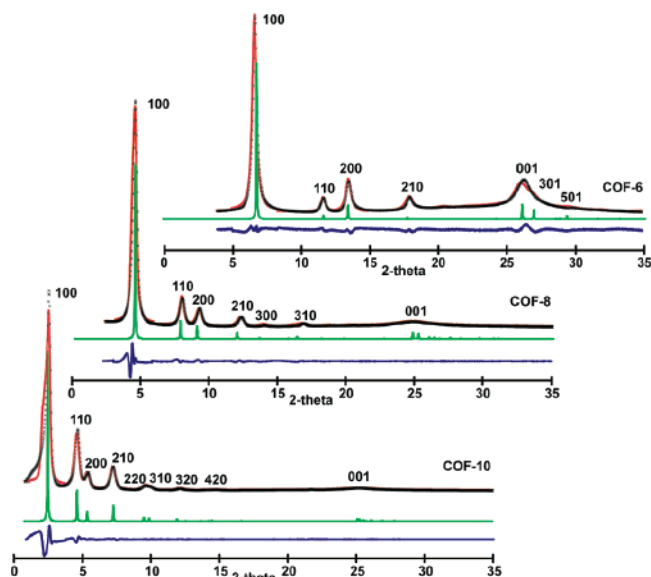


**Figure 2.** Indexed experimental (black) and predicted (green) PXRD patterns for 2D COFs with Le Bail fitting (red) and associated difference plot (blue; observed-fitted) indicated.

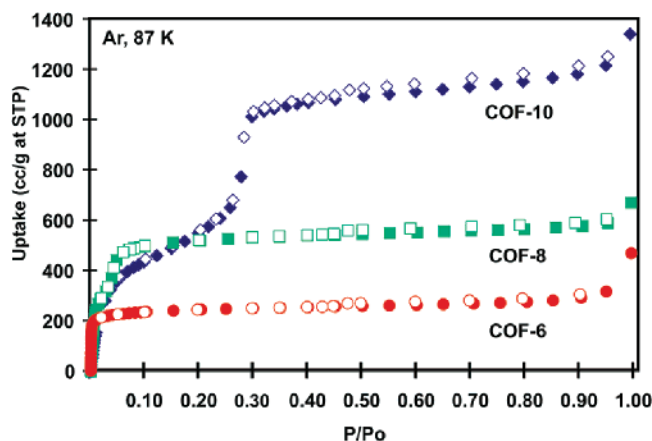


**Figure 3.** Reversible gas adsorption (filled shapes) and desorption (open shapes) isotherms for COFs-6 (red), -8 (green), and -10 (blue).

h leaches starting materials from the pores, and subsequent heating under vacuum ( $85\text{ }^{\circ}\text{C}$ ,  $10^{-5}$  Torr) removes all volatile entities and fully activates the pores. Adsorption of Ar at  $87\text{ K}$  was used to assess the porosity of the COFs (Figure 3). COF-6 exhibits a Type I isotherm indicative of a microporous material, while COFs-8 and -10 display Type IV isotherms, indicating their mesoporosity, with steps occurring at  $P/P_0 = 0.03\text{--}0.05$  and  $0.25\text{--}0.30$ , respectively, corresponding to pore filling and condensation of Ar in 1D pores.<sup>11</sup> Applying the Langmuir model to the appropriate low-pressure regions of the isotherms provided surface areas of  $980$ ,  $1400$ , and  $2080\text{ m}^2\text{ g}^{-1}$  ( $1049$ ,  $968$ , and  $976\text{ m}^2\text{ cm}^{-3}$ ) for COFs-6, -8, and -10, respectively. Pore volumes were determined to be  $0.32$ ,  $0.69$ , and  $1.44\text{ cm}^3\text{ g}^{-1}$  for COFs-6, -8, and -10, respectively. In particular, the value for COF-10 is greater than that typically found for inorganic templated silica materials that also possess hexagonally aligned 1D pores (cf.  $32\text{ }\text{\AA}$  MCM-41,  $1140\text{ m}^2\text{ g}^{-1}$ ,  $0.63\text{ cm}^3\text{ g}^{-1}$ ).<sup>12</sup> The porous structures of COFs were further corroborated by fitting non-local density functional theory models to isotherms to determine pore size distributions that are centered ( $6.4$ ,  $18.7$ ,  $34.1\text{ }\text{\AA}$ ) close to pore diameters from crystal structures ( $8.6$ ,  $16.4$ ,  $31.7$ ).<sup>13</sup> The pore diameter of COF-10 exceeds that of other 2D COFs (COF-1,  $9\text{ }\text{\AA}$ ; COF-18A,  $18\text{ }\text{\AA}$ ; COF-5,  $27\text{ }\text{\AA}$ ),<sup>4,14</sup> and 3D COFs (COF-102 and

$-103$ ,  $12\text{ }\text{\AA}$ ).<sup>5</sup> All isotherms display a small hysteresis between  $P/P_0 = 0.45\text{--}0.90$ , which can be ascribed to interparticle adsorption commonly encountered for particles with plate morphologies.<sup>11</sup>

Low-density and high-porosity materials are promising candidates for gas storage applications. Carbons<sup>15</sup> and polymers of intrinsic microporosity (PIMs)<sup>16</sup> are studied in this regard. The COFs reported here are composed of light elements (B, C, O, H) that are linked by strong covalent bonds to form ordered porous materials with homogeneous pores and high surface areas. In addition, COFs can be reproducibly made using simple and high-yielding syntheses.

In general, it remains a challenge in solid-state chemistry to systematically and predictably vary the metrics and composition of materials. Prior to metal-organic frameworks, and now COFs, only structure-directing agents (SDAs) employed for crystallization of mesoporous silica (e.g., MCM-41) achieved precise metrical control of structure.<sup>17</sup>

**Acknowledgment.** Funded by BASF Ludwigshafen and DOE (DEFG0206ER15813).

**Supporting Information Available:** Detailed synthetic procedures for COFs, modeling techniques and atomic coordinates, FT-IR and MAS NMR spectra, SEM images, TGA traces, atomic coordinates, and PXRD patterns compared to those from **bnn** and **gra** models. This material is available free of charge via the Internet at <http://pubs.acs.org>.

## References

- (1) Yaghi, O. M.; O'Keeffe, M.; Ockwig, N. W.; Chae, H. K.; Eddaoudi, M.; Kim, J. *Nature* **2003**, *423*, 705.
- (2) Kitagawa, S.; Kitaura, R.; Noro, S. *Angew. Chem., Int. Ed.* **2004**, *43*, 2334.
- (3) Eddaoudi, M.; Kim, J.; Rosi, N. J.; Vodak, D. T.; O'Keeffe, M.; Yaghi, O. M. *Science* **2002**, *295*, 469.
- (4) Côté, A. P.; Benin, A. I.; Ockwig, N. W.; O'Keeffe, M.; Matzger, A. J.; Yaghi, O. M. *Science* **2005**, *310*, 1166.
- (5) El-Kaderi, H. M.; Hunt, J. R.; Mendoza-Cortés, J. L.; Côté, A. P.; Taylor, R. E.; O'Keeffe, M.; Yaghi, O. M. *Science* **2007**, *316*, 268.
- (6) Typical synthetic procedure for the synthesis of COF-10: A  $60\text{ mL}$  vial was charged with BPDA ( $0.50\text{ g}$ ,  $2.05\text{ mmol}$ ), HHTP ( $0.44\text{ g}$ ,  $1.37\text{ mmol}$ ), and  $50\text{ mL}$  of a  $1:1\text{ v/v}$  solution of mesitylene/dioxane. The reaction mixture was sonicated for  $30\text{ minutes}$  then heated at  $85\text{ }^{\circ}\text{C}$  for  $3\text{ days}$  to afford a gray powder. The powder was filtered and washed with dry acetone ( $3 \times 20\text{ mL}$ ). The powder was then activated with acetone ( $2 \times 50\text{ mL}$ ) for  $2\text{ days}$  then dried at  $85\text{ }^{\circ}\text{C}$  and  $10^{-5}\text{ Torr}$  for  $12\text{ h}$  to give COF-10 ( $0.53\text{ g}$ ,  $67\%$ ). Calcd for  $\text{C}_{12}\text{H}_6\text{B}_2\text{O}_2$ : C,  $74.68$ ; H,  $3.13$ . Found: C,  $75.08$ ; H,  $3.39$ .
- (7) **gra** and **bnn** are the three letter designators generally given for important common nets as outlined in Reticular Chemistry Structure Resource (RCSR), <http://rcsr.anu.edu.au/>.
- (8) Cerius<sup>2</sup> Modeling Environment, version 4.2; Molecular Simulations Incorporated: San Diego, CA, 1999.
- (9) Larson, A. C.; VonDreele, R. B. *General Structure Analysis System (GSAS)*; Los Alamos National Laboratory Report LAUR 86-748, Los Alamos, NM, 2004. Residual factors: COF-8:  $R_p = 0.0780$ ,  $wR_p = 0.0911$ . COF-10:  $R_p = 0.1383$ ,  $wR_p = 0.2114$ . COF-12:  $R_p = 0.0467$ ,  $wR_p = 0.0632$ .
- (10) It is a multiplicity of possibilities in which COF-8 and -12 can stack and pattern where HHTP stack against BTPA/BPBA (turbostratic disorder) which is crystallographically indistinguishable from PXRD/adsorption data; the tailing to high angle of the (100) lines points to translation faults in the  $xy$  basal planes. This feature does not preclude nor detract from the application of COFs as porous materials. Due to its large unit cell parameters, the (100) line of COF-10 appears at a very low angle ( $2\theta = 2.8^{\circ}$ ) and overlaps with scattering from the X-ray source, resulting in an anomalous tailing to low angle of (100) peak and poorer fit of the Le Bail profile in this region (Figure 2).
- (11) Rouquerol, F.; Rouquerol, J. *Adsorption by Powders and Porous Solids*; Academic Press: London, 2002.
- (12) Kruk, M.; Jaroniec, A.; Sayari, J. *J. Phys. Chem. B* **1997**, *101*, 583–589.
- (13) Schumacher, K.; Ravikovich, P. I.; Chesne, A. D.; Neimark, A. V.; Unger, K. K.; *Langmuir* **2000**, *16*, 4648.
- (14) COF-18A was prepared using similar procedures to that COFs-1 and -5: Tilford, W. R.; Gemmil, W. R.; zur Loye, H.-C.; Lavigne, J. J. *Chem. Mater.* **2006**, *18*, 5296.
- (15) Texier-Mandoki, N.; Dentzer, J.; Piquero, T.; Saadallah, S.; David, P.; Vix-Guterl, C. *Carbon* **2004**, *42*, 2744.
- (16) Ghanem, B. S.; Msayib, K. J.; McKeown, N. B.; Harris, K. D. M.; Pan, Z.; Budd, P. M.; Butler, A.; Selbie, J.; Book, D.; Walton, A. *Chem. Commun.* **2007**, 67.
- (17) Thommes, M. In *Nanoporous Materials Science and Engineering*; Lu, G. Q., Zhao, X. S., Eds.; Imperial College Press: London, 2004.

JA0751781